the UTC is equipped with an additional back wall due to the building wall conditions. An air gap between the UTC back wall and the building wall results from this special construction.

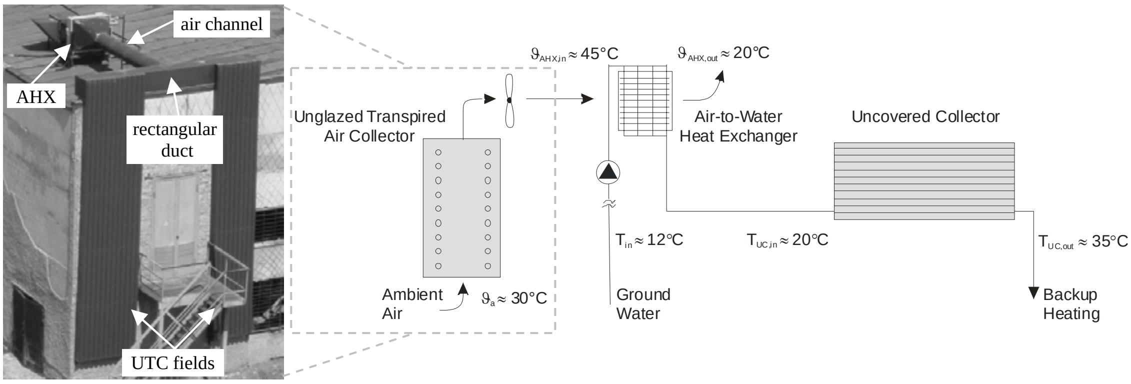

Fig. 2. Experimental setup at a heat plant in Bishkek (Kyrgyzstan) (left) and the scheme of a serially connected multicomponent system with exemplary temperatures (right).

2. Extended numerical model for UTCs

Due to the unconventional boundary conditions of the application an extended numerical model was developed and compared to measurement data collected in Bishkek. The model was derived from existing models for facade-mounted UTCs using the building wall as back wall for the collector [4]. The temperatures of the absorber, the back wall of the collector, the building wall and the plenum are assumed to be uniform, therefore a homogenous flow across the whole collector area is presumed. The quality of these assumptions depends on the air flow rate: With higher flow rates, the difference between the temperatures at the top and bottom areas of the collector increases because the suction velocity at the top area of the collector is greater than at the bottom [5].

In the following, a 9x1-knot model is introduced consisting of three energy balance equations, rate and efficiency equations. The resulting system of equations can be solved numerically, thus determining the outlet temperature of the collector T_{out}. Eqs. (1-3) describe the thermal performance of the UTC based on the energy balances of the perforated absorber, the back wall of the collector and the building wall (cf. Fig. 3).[2] The capacities of the absorber and the back wall are neglected due to their low masses.

Rate equations for the energy flows are required in order to solve the energy balance equations. According to [6], the solar radiation absorbed by the collector $Q_{abs,col}$, the energy flux between collector and back wall $\dot{Q}_{rad,col-back}$ and losses to the environment via radiation $\dot{Q}_{rad,col-sur}$ can be calculated directly (eqs. 4-6). The dependency of the absorption coefficient on the angle of incidence is approximated by a correlation typical for plane black surfaces [6] because it is unknown for corrugated UTCs, so far.

For corrugated transpired solar collectors, convective losses to the surrounding must not be neglected. Empirical studies of large UTC systems showed that the efficiency of UTCs is depending on the wind speed [7, 8]. Therefore, the Nusselt number Nu_{lost} was determined numerically and experimentally [9]. Depending on the operating conditions, attached or separated boundary layers can occur at the absorber plate. Thermal losses for separated boundary layers are considerably greater than for attached layers. For both cases, [9] determines a specific Nusselt number correlation. For average suction face velocities $\mathrm{v}_0 \geq 6{,}93 \cdot \lambda^{-1}\sqrt{\hat{y}\nu_{air}\mathrm{v}_w}$ eq. (8) has to be applied, otherwise eq. (9).

[2] The labelling convention for heat flows is $\dot{Q}_{Mode,\,from-to}$, where *Mode* denotes the heat transfer mechanism (*conv* for convection, *rad* for radiation, *abs* for absorption, *cap* for capacity) and *from*/*to* describe the source/destination of heat transfer, respectively.

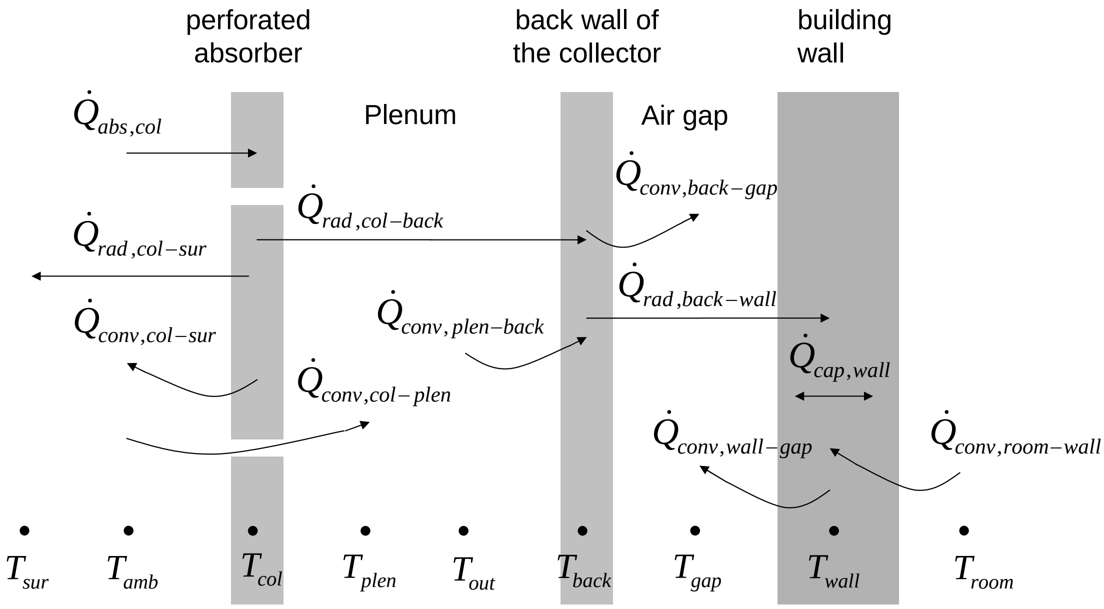

Fig. 3. Heat flows at the perforated absorber, the back wall of the collector and the building wall. The bottom line represents the 9 temperature knots.

$$\dot{Q}_{abs,col} = \dot{Q}_{rad,col-back} + \dot{Q}_{rad,col-sur} + \dot{Q}_{conv,col-sur} + \dot{Q}_{conv,col-plen} \tag{1}$$

$$\dot{Q}_{rad,col-back} + \dot{Q}_{conv,plen-back} = \dot{Q}_{conv,back-gap} + \dot{Q}_{rad,back-wall} \tag{2}$$

$$\dot{Q}_{cap,wall} = \dot{Q}_{rad,back-wall} - \dot{Q}_{conv,wall-gap} + \dot{Q}_{conv,room-wall} \tag{3}$$

$$\begin{aligned}\dot{Q}_{abs,col} &= G_t \cdot A \cdot \alpha \cdot \frac{\alpha(\Theta)}{\alpha_\perp} \\ &= G_t \cdot A \cdot \alpha \cdot \left\{ \begin{aligned} &1 + 2,0345 \cdot 10^{-3} \frac{\Theta}{Grad} - 1,990 \cdot 10^{-4} \cdot \left(\frac{\Theta}{Grad}\right)^2 \\ &+ 5,324 \cdot 10^{-6} \cdot \left(\frac{\Theta}{Grad}\right)^3 - 4,799 \cdot 10^{-8} \cdot \left(\frac{\Theta}{Grad}\right)^4 \end{aligned} \right\}\end{aligned} \tag{4}$$

$$\dot{Q}_{rad,col-back} = \frac{A \cdot \sigma \left(T_{col}^4 - T_{back}^4\right)}{\frac{1}{\varepsilon_{col,plen}} + \frac{1}{\varepsilon_{back}} - 1} \tag{5}$$

$$\dot{Q}_{rad,col-sur} = A \cdot (1-\kappa) \cdot \sigma \cdot \varepsilon_{col} \cdot \left(T_{col}^4 - T_{sur}^4\right) \tag{6}$$

$$\dot{Q}_{conv,col-sur} = h_{col-sur} A\left(T_{col} - T_{amb}\right) = \frac{\mathrm{Nu}_{lost} \cdot k_{air}}{H} A\left(T_{col} - T_{amb}\right) \tag{7}$$

$$\mathrm{Nu}_{lost,att} = 0,82 \frac{\rho_{air} c_{p,air} \mathrm{v}_w \nu_{air}}{k_{air} \mathrm{v}_o} \left[1 + 0,81 \left(\frac{\hat{y}}{\lambda}\right)^{0,5}\right] \tag{8}$$

$$\mathrm{Nu}_{lost,sep} = 2,05 \left(\frac{\hat{y}}{\lambda}\right)^{1,40} \mathrm{Re}_{lost}^{\;1,63} \tag{9}$$

As the ambient air passes over and through the absorber, it is heated up by the convective heat flow from the collector into the plenum. Thus, this heat flow can be calculated by eq. (10).

$$\dot{Q}_{conv,col-plen} = \dot{m}_{air} c_{p,air} \left(T_{plen} - T_{amb}\right) \tag{10}$$

Eq. (2) is the energy balance for the back wall of the collector. Because of the small thickness and the low thermal resistance the back wall is modelled with a single temperature knot and its capacity is neglected.

While the air is passing through the perforated absorber it is heated up to the temperature T_{plen}. If T_{back} is lower than T_{plen} the air flow in the collector to the top of the plenum is then cooled down to the outlet temperature T_{out} by a convective heat flow to the back wall. This heat flow can be expressed by the following eq. (11):

$$\dot{Q}_{conv,plen-back} = \dot{m} \cdot c_{p,air} \cdot \left(T_{plen} - T_{out}\right) \tag{11}$$

The heat flows $\dot{Q}_{conv,plen-back}$ and $\dot{Q}_{conv,back-gap}$ can also be expressed in terms of their heat transfer coefficients:

$$\dot{Q}_{conv,plen-back} = h_{plen-back} A\left(T_{out} - T_{back}\right) = \frac{\mathrm{Nu}_{plen-back} \cdot k_{air}}{H} A\left(T_{out} - T_{back}\right) \tag{12}$$

$$\dot{Q}_{conv,back-gap} = h_{back-gap} A\left(T_{back} - T_{gap}\right) = \frac{\mathrm{Nu}_{free} \cdot k_{air}}{H} A\left(T_{back} - T_{gap}\right) \tag{13}$$

So far no systematic investigations have been carried out regarding the properties of the air flow in the plenum. Therefore, no specific heat transfer function exists so that an approximation for forced convection at parallel flat-plate airflows is applied. Free convection from the back wall of the collector to the air in the plenum is expressed by adapting known correlations for streams hitting vertically on a plane [10].

The radiation heat flow between the back wall of the collector and the building wall can be calculated analogous to eq. (5).

As shown in experimental results [11], the heat capacity of the building wall (cf. eq. (3)) can not be neglected. The capacity heat flow is calculated by eq. (14).

$$\dot{Q}_{cap,wall} = m_{wall} c_{p,wall} \dot{T}_{wall} \tag{14}$$

The heat flows $\dot{Q}_{conv,wall-gap}$ and $\dot{Q}_{conv,room-wall}$ can be determined analogous to $\dot{Q}_{conv,back-gap}$.

For solving the system of equations in eq. (15) the heat exchange effectiveness ε_{HX} of the absorber is defined. ε_{HX} can also be calculated by eq. (16) using the appropriate heat transfer coefficient. For the convectional heat transfer from the collector plate to the air flow in the plenum a Nusselt number is applied that was derived experimentally [12], cf. eq (17).

$$\varepsilon_{HX} = \left(T_{plen} - T_{amb}\right) / \left(T_{col} - T_{amb}\right) \tag{15}$$

$$\varepsilon_{HX} = 1 - \exp\left(-\frac{\mathrm{Nu}_{col-plen} \cdot k_{air} \cdot (1-\kappa)}{D \cdot \rho_{air} \cdot \mathrm{v}_0 \cdot c_{p,air}}\right) \tag{16}$$

$$Nu_{col-plen} = 2,75 \cdot \left(\frac{P}{D}\right)^{-1,2} \mathrm{Re}_D^{0,43} \tag{17}$$

3. Selected simulation results

The presented UTC model was implemented into the simulation environment TRNSYS. Calculations have been carried out for conditions as they can be found in the application in Bishkek using values from literature or manufacturer`s specifications for absorption coefficients, emissivities etc.. Fig. 4 shows the simulated efficiency and air temperature rise of the unglazed transpired collector as a function of air flow rate for no wind and a wind speed of 5m/s. Especially for low specific air flow rates in the range of $100 m^3h^{-1}m^{-2}$ the collector efficiency varies significantly depending on the wind conditions, which corresponds with experimental data. Further analysis of the modelled heat flows with low air flow rates and a wind speed of 5m/s showed that losses by convective heat flow are significant and in the range of heat losses by radiation (cf. Table 1).

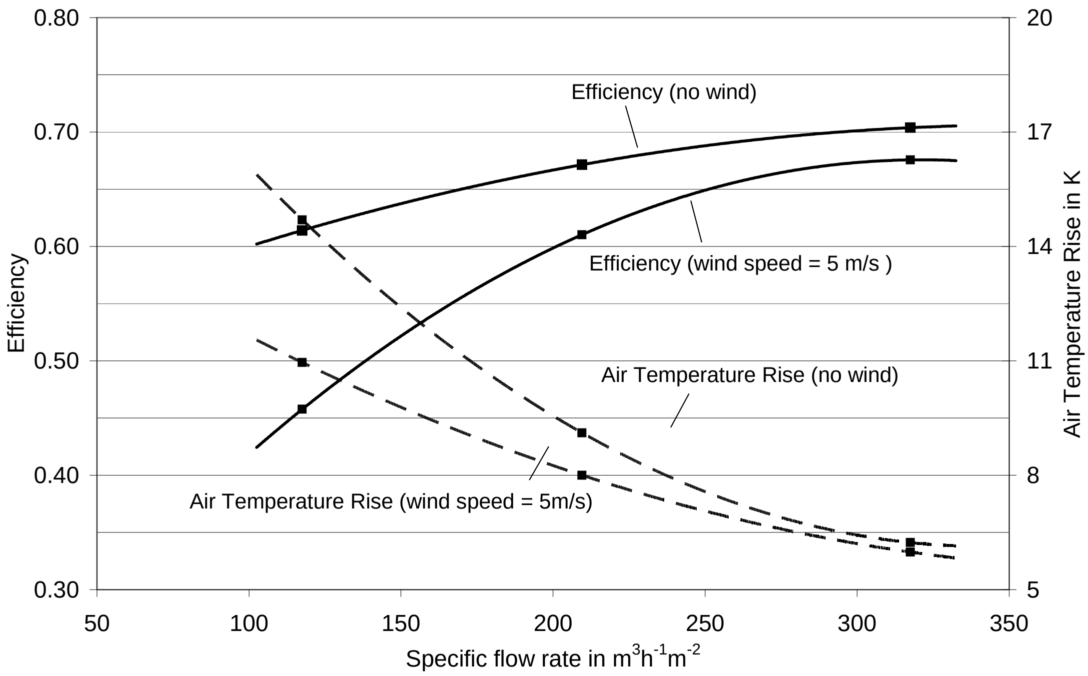

Fig. 4. Efficiency (left axis) and air temperature rise (right axis) of an unglazed transpired collector as a function of air flow rate for no wind and a wind speed of 5m/s (global irradiation = 900Wm-2, ambient temperature = 32°C and sky temperature = 7°C).

Table 1. Heat flow ratios of the perforated absorber for low air flow rates (120$m^3h^{-1}m^{-2}$).

v_w	$\dot{Q}_{abs}$	$\dot{Q}_{rad,col-sur}$	$\dot{Q}_{conv,col-sur}$	$\dot{Q}_{conv,col-plen}$	$\dot{Q}_{rad,col-back}$
0 ms^{-1}	100 %	25,4 %	0 %	67,7 %	6,9 %
5 ms^{-1}	100 %	20,6 %	23,9 %	50,5 %	5,0 %

4. Conclusions and Outlook

An extended numerical model has been developed for unglazed transpired air collectors with unusual operating conditions. The model covers already known standard applications as well as specific features of the collector. Especially, convective losses from the collector to the surrounding, the dependency of the absorption coefficient on the angle of incidence and the capacity of the building wall are considered. The simulation results are consistent with first experimental data collected in Bishkek. Thereby values of the absorption coefficients, the emissivities etc. have been taken from literature or manufacturer`s specifications. In a next step the model parameters will be determined using experimental data.

Acknowledgements

The authors would like to express their gratitude to the following institutions for their financial and logistical support: The VolkswagenStiftung (Germany) which funds the research project, the Center of the Problems of Unconventional and Renewable Energy Sources (Kyrgyzstan), the Kyrgyz Technical University in Bishkek, and the district heating net operator Bishkekteploenergo (Kyrgyzstan).

Nomenclature

A = collector face area, m^2

$c_{p,air}$ = specific heat of air, $J\left(kgK\right)^{-1}$

$c_{p,wall}$ = specific capacity of the building wall, $J\left(kgK\right)^{-1}$

D = collector hole diameter, m

G_t = radiation incident on collector, W/m^2

H = height of the air collector, m

h = heat transfer coefficient, $Wm^{-2}K^{-1}$

k_{air} = thermal conductivity of air, $Wm^{-1}K^{-1}$

m_{wall} = mass of building wall, kg

$\dot{m}_{air}$ = mass flow rate of air, *kg/s*

Nu_{lost} = Nussel number for corrugated plates

$Nu_{lost,att}$ = Nussel number for corrugated plates in attached flow

$Nu_{lost,sep}$ = Nussel number for corrugated plates in separated flow

$Nu_{plen-back}$ =Nussel number for forced convection

Nu_{free} = Nussel number for free convection

$\dot{Q}_{Mode,\,from-to}$ = heat flow, *W*

$\dot{Q}_{cap,wall}$ = heat capacity flow of building wall, *W*

Re = Reynolds number

T_{amb} = ambient air temperature, *K*

T_{back} = backside plate temperature, *K*

T_{col} = collector surface temperature, *K*

T_{gap} = air temperature of the air gap, *K*

T_{out} = collector outlet temperature, *K*

T_{plen} = plenum air temperature, *K*

T_{room} = room temperature, *K*

T_{sky} = sky temperature, *K*

$T_{sur} = \left\{0,5\left(T_{sky}^4 + T_{gnd}^4\right)\right\}^{0,25}$ = surroundings temperature, *K*

$\dot{T}_{wall}$ = alteration of the wall temperature, *K/s*

$\dot{V}_{air}$ = air flow rate, *m³/s*

v_0 = average suction face velocity, *m/s*

v_w = wind speed, *m/s*

$\hat{y}$ = amplitude of corrugations, *m*

α = absorption coefficient of collector

$\alpha(\Theta)/\alpha_\perp$ = dependency of the absorption coefficient on the angle of incidence

σ = Stefan-Boltzmann constant

ε_{back} = emissivity of backside of the collector

ε_{col} = collector emissivity

$\varepsilon_{col,plen}$ = collector emissivity towards the plenum

ε_{HX} = heat exchanger effectiveness of collector

ε_{wall} = emissivity of the building wall

κ = collector porosity

λ = wavelenght of corrugations, *m*

ν_{air} = kinematic viscosity of air, m^2/s

ρ_{air} = density of air, kg/m^3

Θ = angle of incidence, °

References

[1] C.F. Kutscher, C.B. Christensen, G.M. Barker (1991): Unglazed transpired Solar Collectors: An analytical Model and Test Results, Proceedings of ISES, 1991, pp. 1245-1250

[2] C.F. Kutscher, C.B. Christensen, G.M. Barker (1993): Unglazed transpired Solar Collectors: Heat loss theory, Journal of Solar Engineering (Trans ASME), Vol. 115 No 3, pp. 182-188

[3] E. Frank, K. Vajen, A. Obozov, V. Borodin (2006): Preheating for a District Heating Net with a Multicomponent Solar Thermal System, Proceedings of EuroSun, Glasgow

[4] D.N. Summers (1995): Thermal Simulation and Economic Assessment of Unglazed Transpired Collector Systems, M.A.Sc. Thesis, University of Wisconsin-Madison, USA

[5] L.H. Gunnewiek, E. Brundrett, K.G.T. Hollands (1996): Flow distribution in unglazed transpired-plate solar air heaters of large area, Solar Energy Vol.58 pp. 227-237

[6] J.A. Duffie, W.A. Beckman (1991): Solar Engineering of Thermal Processes, John Wiley & Sons, New York

[7] S.R. Hasting (Ed.), O. Morck (Ed.) (2000): Solar Air Systems - A Design Handbook, London: James & James Ltd

[8] A.P. Brunger (Ed.) (1999): Low Cost, High Performance Solar Air-Heating Systems Using Perforated Absorbers, IEA Solar Heating and Cooling Report No. SHC.T14.Air:I; Final Report of Task 14 Air Systems Working Group

[9] K. Gawlik, C.F. Kutscher (2002): Wind Heat Loss From Corrugated, Transpired Solar Collectors, Journal of Solar Energy Engineering, V 124, Issue 3, pp. 256-261

[10] Verein Deutscher Ingenieure (1994): VDI-Wärmeatlas, VDI-Verlag, 7. Auflage

[11] C. Budig (2005): Experimentelle Untersuchung und Modellierung eines unabgedeckten durchströmten Luftkollektors, diploma thesis, Institut für thermische Energietechnik, Universität Kassel (Germany)

[12] C.F. Kutscher (1994): Heat Exchange Effectiveness and Pressure Drop for Air Flow through Perforated Plates with and without Crosswind, Journal of Heat Transfer (Trans ASME), Vol. 116, pp. 391-399